Groundwater Flow Modeling and Adopting a Different Approach in Dealing Pumping Wells

Mohammad Javad Zeynali[a]*, Mohammad Nazeri Tahroudi[b], Omolbani Mohammadrezapour[c]

[a]Assistant Professor, Department of Economic Sciences and Water Engineering, University of Torbat Heydarieh, Torbat-e Heydarieh, Iran.
[b]Asistant Professor, Department of Water Engineering, Lorestan University, Khorramabad, Iran.
[c]Associate Professor, Department of Water Engineering, Gorgan University of Agricultural Sciences and Natural Resources, Gorgan, Iran.

*Corresponding Author E-mail address: mj.zeynali@torbath.ac.ir

Abstract

In groundwater flow modeling, as in any modeling problem, a certain amount of error is inevitable. Recharge or discharge wells, acting as point sources or sinks, play a key role in modeling accuracy, and the way they are treated can either reduce or increase errors. In this study, two approaches were investigated: first, transferring the well to the nearest node in its neighborhood, and second, distributing the pumping rate of the well among the closest nodes. A hypothetical aquifer was examined under two conditions-unconfined and confined-and using both triangular and square meshes. The results indicated that simplifying the model by moving the pumping well to the nearest node is justified only for unconfined aquifers with triangular meshes. For other cases-including unconfined aquifers with square meshes and confined aquifers with either mesh-the second approach is recommended, as it significantly reduces errors in groundwater flow modeling. These findings can also be generalized to real aquifer studies. Quantitative results show that Approach 2 consistently reduces modeling errors: for unconfined aquifers, MAE values are below 0.03 for both mesh types, whereas confined aquifers exhibit larger reductions, particularly with triangular meshes, where MAE reaches 0.38 and maximum errors up to 1.17. These results highlight the robustness of Approach 2 across different mesh configurations and aquifer conditions, providing an effective and reliable numerical tool for groundwater modeling.

Keywords: Pumping Rate Separation, Pumping Well Location, Rectangular mesh, Transfer, Triangular mesh.

1. Introduction

Groundwater is one of the most important sources of freshwater across the world and the lives of many people depend on it. Because these resources are located underneath the Earth's top crust, therefore, are poorly monitored and managed. It can be said that these resources are more difficult to investigate and manage than surface waters. but, Groundwater flow modeling helps us to better understand the behavior of groundwater flow and the fate of pollutants in groundwater.

A well-constructed groundwater model provides benefits to multiple stakeholders. Modelers benefit from an accurate and validated computational framework that allows them to test hypotheses and explore system behavior. Hydrogeologists gain insights into aquifer dynamics, recharge and discharge patterns, and flow paths. Remediation engineers can use the model to design and optimize groundwater remediation strategies, predict contaminant transport, and evaluate the effectiveness of intervention measures. In summary, a reliable groundwater model supports decision-making across modeling, hydrogeology, and remediation applications.

A well-developed groundwater flow model offers substantial benefits to a wide range of stakeholders. For modelers, it provides a robust computational framework for testing conceptual models, conducting sensitivity analyses, and exploring system behavior under various boundary conditions and stress scenarios. Hydrogeologists use groundwater models to gain insight into aquifer properties, hydraulic connectivity, recharge mechanisms, and groundwater flow paths. Furthermore, environmental and remediation engineers rely on these models to design and optimize remediation strategies, assess contaminant plume migration, and evaluate the effectiveness of management and intervention measures. Consequently, reliable groundwater modeling supports informed decision-making in water resource management, environmental protection, and engineering applications (Reilly and Harbaugh, 2004).

Despite their wide applicability, numerical groundwater flow models are inherently subject to uncertainties and errors. These errors may arise from incomplete conceptualization of the aquifer system, uncertainty in hydraulic parameters, simplifications in boundary conditions, or numerical discretization. Among the various sources of modeling error, the representation of pumping and recharge wells plays a particularly important role. Wells are typically treated as point sources or sinks within the numerical domain, and the manner in which their locations and pumping rates are incorporated into the model can significantly influence simulation accuracy (Koch et al., 2020).

In many groundwater modeling studies, wells are assigned to the nearest computational node or cell to simplify model implementation. While this approach may be computationally convenient, it can introduce significant numerical errors, especially when the well location does not coincide with the mesh geometry or when coarse discretization is used. Alternatively, distributing the pumping rate of a well among multiple neighboring nodes or cells has been proposed as a means of better representing the physical influence of the well on the surrounding groundwater flow field. However, the effectiveness of these approaches depends on factors such as aquifer type, mesh structure, and model discretization (Lozano Hernández et al., 2024).

Given the importance of accurately representing pumping wells in groundwater flow models, a systematic evaluation of different well-treatment approaches is essential.

The numerical methods such as finite difference method (FDM) and finite element method (FEM) and meshfree are more commonly used by researchers for groundwater flow modeling, contaminant transport, and groundwater remediation. Many researchers have used numerical methods for groundwater modeling (Akbarpour et al., 2020), contaminant transport (Zeynali et al., 2022), and groundwater remediation (Zeynali et al, 2022, Zeynali et al., 2024, Zeynali et al., 2024). Jafarzadeh et al. (2023) investigated the effects of scheme type, time step, and error threshold on the stability of numerical simulations in groundwater modeling. Their results demonstrated that the finite element (FE) model is capable of accurately simulating groundwater fluctuations, even in real-world problems with higher levels of complexity. In a real-world application, Singh and Pathania (2025) implemented the GFDM model for a large unconfined aquifer in the Middle Ganga Plain, Bihar, India, covering an area of 11,470 km². The aquifer boundaries include three rivers and a hill, and extensive groundwater withdrawals are represented by 2,262 pumping wells assigned to all field nodes.

The hydraulic head solutions obtained using the GFDM model closely matched the MODFLOW results, indicating that the proposed approach can reliably simulate complex aquifer systems under realistic conditions. Vellando et al. (2020) developed a nonlinear MATLAB-based finite-element model, FLUMP, to simulate flow in unconfined, saturated, heterogeneous, and anisotropic porous media, incorporating tools to evaluate free-surface flow through the conservation of mass. The study compared FLUMP with the widely used finite-difference software MODFLOW, using Wang's benchmark problem of a lowering reservoir for validation and subsequently applying both models to the Barces Watershed, a real-world case extensively monitored over the last decade. Their findings highlighted the

strengths and limitations of FEM versus FDM in simulating groundwater flow through porous media. While FLUMP is not intended to replace MODFLOW as a de facto standard, the comparison demonstrated the benefits of the finite-element approach, particularly in handling complex heterogeneous and anisotropic aquifers, and emphasized how FEM and FDM can complement each other in hydrogeological modeling.

To illustrate how numerical methods operate, several studies analyze both hypothetical and real aquifers. Some researchers investigate hypothetical aquifers (Kumar et al., 2015, Mategaonkar et al., 2018, Guneshwor et al., 2018) while others examine real aquifers (Mohtashami et al., 2017) and some have studied both types of aquifers in their research (Eldho and Swathi, 2018, Ghafouri and Darabi, 2007). Also, in optimization problems where the optimal location of pumping wells in the Pump-and-Treat (PAT) system is important, the location of the pumping wells is only placed on the nodes (Sharief et al., 2012).

To our best acknowledge, it can be explain that in groundwater flow modeling in hypothetical aquifers, pumping wells are always considered to covered by the nodes. Also, in real aquifers, after using the regular distribution of nodes in finite difference or finite element methods, the wells (as a recharge or discharge) are transferred to the nearest node. Also, if several pumping wells are located on one node, the pumping flow rates of these wells are summed together. Given that there is always a percentage of error in groundwater flow modeling, this approach can also add to this error. Besides, suppose an aquifer is represented by a square grid with four corner nodes, each side measuring 500 m, and a well-placed exactly at the square's center; in this case, the well position can be mapped to any of the four neighboring nodes, which implies a displacement of 354 m. Clearly, transferring the well from one point to another can increase modeling error.

Moreover, using a denser grid raises computational cost, and it is not feasible to guarantee that the desired well coincides with a grid node. This issue is also raised in the discussion of contaminant transport modeling and determining the location of pumping wells

for PAT system. This means that pumping wells must be covered by nodes, while pumping wells in another location may be more efficient in pumping pollution. Therefore, in the present study, a different approach is adopted in dealing with the method of determining the location of pumping wells, which will reduce the amount of modeling error.

2. Materials and Methods
2.1. Case Study

In this study, a hypothetical auifer with length of the 1500 and its width equal to 1000 m is considered (Fig. 1). The hydrogeologic parameters for the aquifer are presented in Table 1. There is a lake with rate of seepage of 0.009 m/d in Zone A. Also, top of Zones A and bottom of Zone C are considered to be recharged and discharsed at a rate of 0.2 and 0.01 m/d, respectively (Fig. 1). The flow model has constant head conditions on its left and right boundaries with 100 and 98 m, respectively and the other boundares are the no-flow boundary. There are four pumping wells and one recharge well in this hypothetical auifer.

Four pumping wells are located on (400,770), (700,650), (1250,350) and (1230,725) coordinate with the rate of pumping of 600, 500, 400 and 300 m^3/day respectively and the recharge well is located on (200,200) coordinate with the rate of recharge of 500 m^3/day.

Three different hydraulic conductivities can be observed in the hypothetical aquifer domain. Therefore, the model domain must be discretized such that the element boundaries coincide with the interfaces between the zones. This issue is well illustrated in Fig. 2 (Istok, 1989).
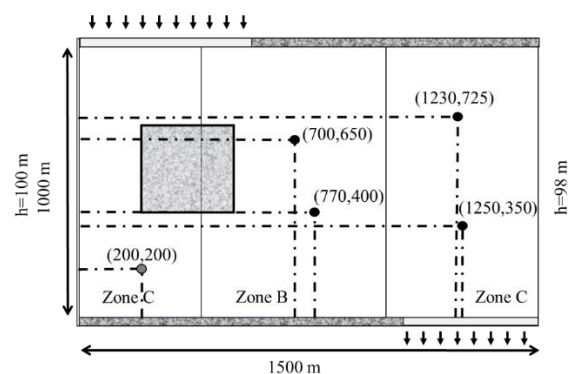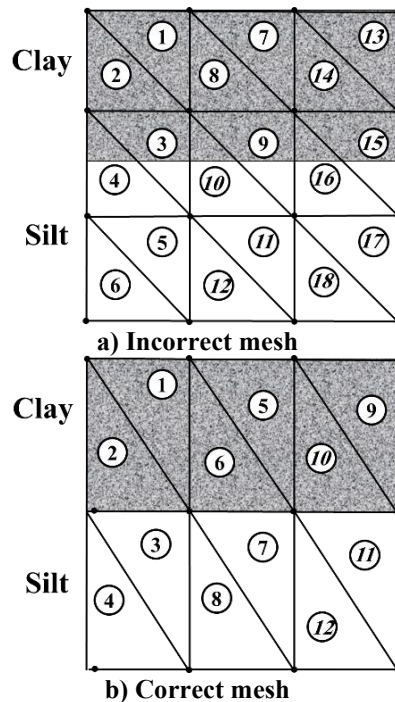

Fig. 1. Hypothetical aquifer configuration

Table 1. Hydrogeologic data used for flow model.

Properties	Zone A	Zone B	Zone C
Hydrolic Conductivity (Kx)	5	4	3
Hydrolic Conductivity (Kx)	8	5	2
Specific Yield	0.15	0.15	0.15
Aquifer Thickness	100	100	100
Transmissivity (Tx)	500	400	300
Transmissivity (Ty)	800	500	200
Storage Coefficient	0.15	0.15	0.15

Considering this issue, the gridding was done in such a way that nodes 1 to 55 were placed in Zone A, nodes 56 to 121 in Zone B, and nodes 122 to 176 in Zone 3. Also, considering this type of gridding, the lake boundary located in Zone A corresponds to nodes 27 to 30, 38 to 41, 49 to 52, and 60 to 63. Fig. 3 and Fig. 4 show the triangular and rectangular (square) gridding of the model domain. As can be seen in these figures, one of the wells is located exactly on node number 25, but the other wells are not exactly aligned on the nodes.

Also, the inflow to the aquifer occurs from the boundary of Zone A and from nodes 22, 33, 44, 55, and 66, and the outflow from the aquifer occurs from the boundary of Zone C and from nodes 122, 133, 144, and 155. The inflow and outflow rates are 0.2 and 0.01 m/day, respectively.

The numerical simulations were performed using MATLAB. A time discretization scheme was employed, and a convergence tolerance of 0.01 was used to ensure accurate solution of the model. The model domain was discretized using triangular and square elements, and pumping wells were treated according to the proposed approaches.

a) Incorrect mesh

b) Correct mesh

Fig. 2. Model domain mesh
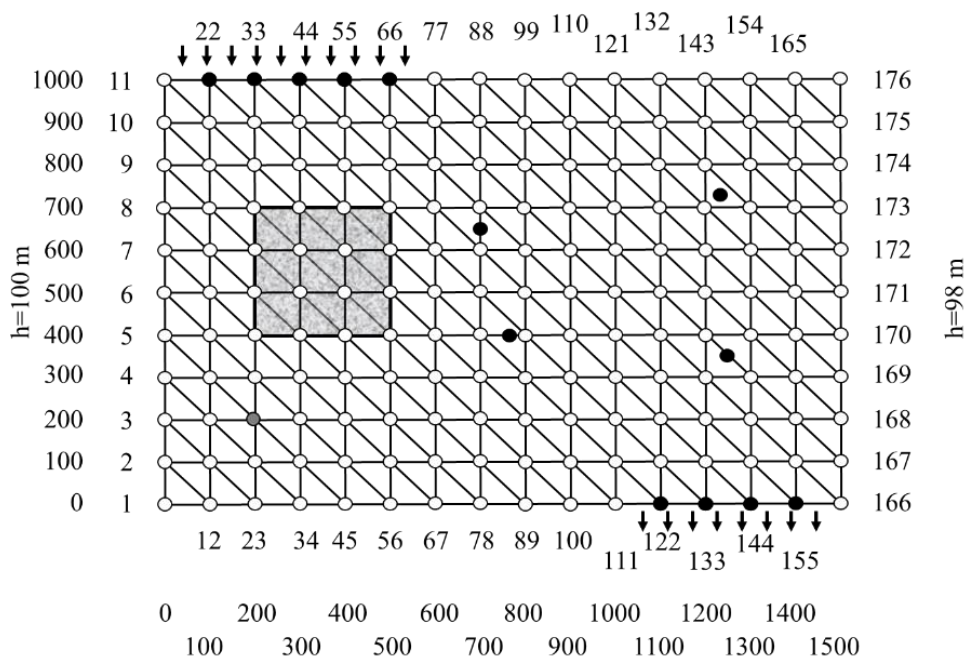
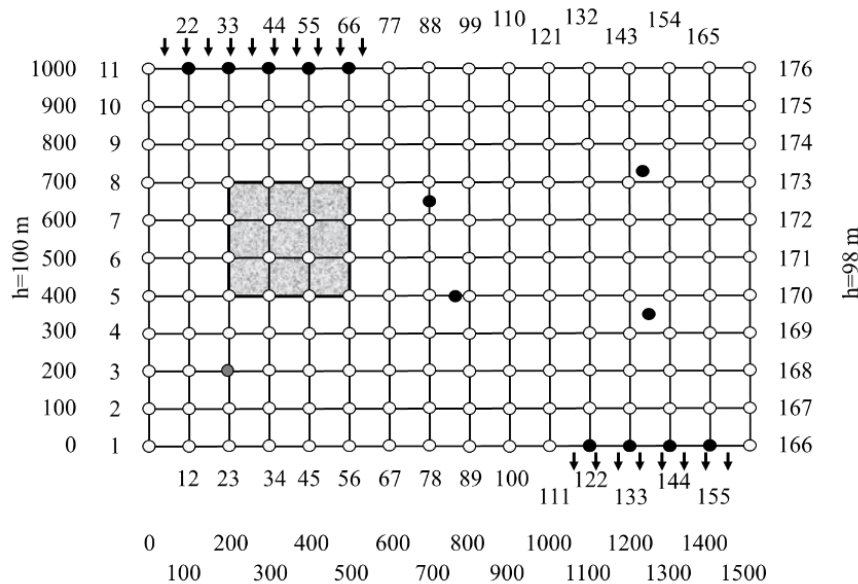**Fig. 3**. Triangular mesh of the model domain

Fig. 4. Rectangular (square) mesh of the model domain

2.2. Approach 1 (transfer the location of the well)

In this approach, which is the same as the simple approach; after creating the mesh, each of the wells that did not exactly coincide with a node is moved to the nearest neighboring node. Therefore, in the triangular mesh, wells numbered 1 to 4 are placed on nodes 93, 84, 147, and 140 and the coordinates of these nodes are (400,800), (600,700), (300,1300), and (700,1200), respectively. Since well No. 2 was equidistant from nodes 84 and 85, either of these nodes could have been selected. Also, well number 3, which is located exactly on the edge of two elements, can be moved to any of its two neighboring nodes(nodes number 136, 137, 147 or 148), and finally the location of the wells in the triangular mesh will be as Fig 5. The same applies to regular rectangular (squar) mesh.
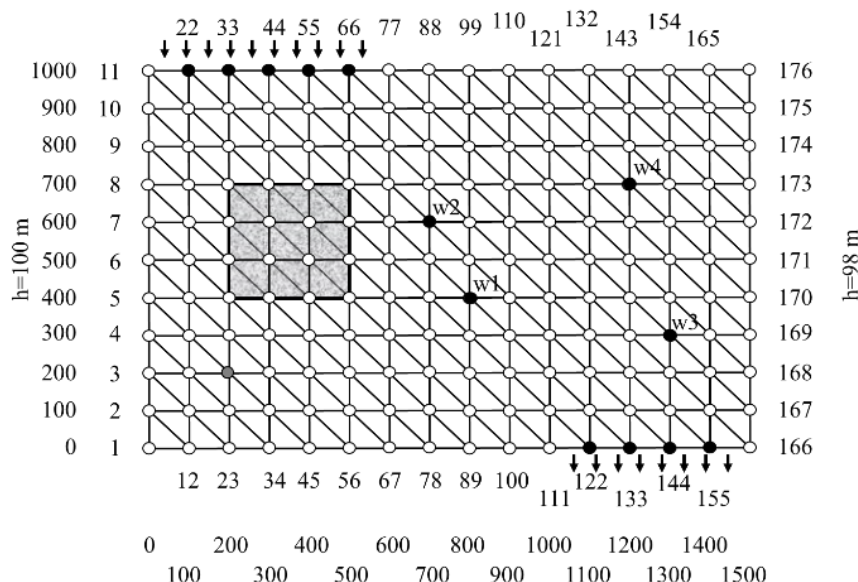

Fig. 5. Triangular mesh and the location of wells in approach 1

2.3. Approach 2 (pumping rate separation)

As mentioned, when groundwater flow equations are solved, cases involving discharge or recharge wells within the model domain are inevitably encountered. Although these wells are much easier to code due to the point nature of the discharge or recharge factor. However, when discretizing the model domain, these factors can be seen in three

cases: 1- The location of the well exactly coincide with a node of the element. 2- The location of the well is located on an edge of the element. 3- The well is located inside the element.

In each of the above cases, the simplest approach is to transfer the location of the well to the nearest node, given the coordinates of the well location. However, a more detailed approach to dealing with each of the above cases is discussed below.

$$2A^e = (x_i y_j - x_j y_i) + (x_m y_i - x_i y_m) + (x_j y_m - x_m y_j) \tag{1}$$

$$N_i^e(x,y) = \frac{1}{2A^e}\left[(x_j y_m - x_m y_j) + (y_j - y_m)x + (x_m - x_j)y\right]$$

$$N_j^e(x,y) = \frac{1}{2A^e}\left[(x_m y_i - x_i y_m) + (y_m - y_i)x + (x_i - x_m)y\right] \tag{2}$$

$$N_m^e(x,y) = \frac{1}{2A^e}\left[(x_i y_j - x_j y_i) + (y_i - y_j)x + (x_j - x_i)y\right]$$

Suppose a well with a pumping rate of 12 m³/day is located exactly at node j and using equation (2) for each of the shape functions we will have:

$$N_i^e(x,y) = \frac{1}{16}\left[((4)(4) - (2)(0)) + (0 - 4)x + (2 - 4)y\right]$$

$$\Rightarrow N_i^e(4,0) = \frac{1}{16}\left[16 - 4x - 2y\right] = \frac{1}{16}\left[16 - 4(4) - 2(0)\right] = 0$$

$$N_j^e(x,y) = \frac{1}{16}\left[((2)(0) - (0)(4)) + (4 - 0)x + (0 - 2)y\right]$$

$$\Rightarrow N_j^e(4,0) = \frac{1}{16}\left[0 + 4x - 2y\right] = \frac{1}{16}\left[0 + 4(4) - 2(0)\right] = \frac{16}{16} = 1$$

$$N_m^e(x,y) = \frac{1}{16}\left[((0)(0) - (4)(0)) + (0 - 0)x + (4 - 0)y\right]$$

$$\Rightarrow N_m^e(4,0) = \frac{1}{16}\left[0 + 0 + 4y\right] = \frac{1}{16}\left[0 + 0(4) + 4(0)\right] = 0$$

So, the pumping rate for three nodes will be equal to:

$$Q = 12\begin{Bmatrix} 0 \\ 1 \\ 0 \end{Bmatrix} = \begin{Bmatrix} 0 \\ 12 \\ 0 \end{Bmatrix} \begin{matrix} i \\ j \\ m \end{matrix}$$

Now, the second case is considered, in which the well is assumed to be located on an edge of the element. The well is located on the edge on both sides of which there are nodes j and m and its coordinate is (3,2). In this case, according to equation (2), for each of the shape functions we will have:

$$N_i^e(x,y) = \frac{1}{16}\left[((4)(4) - (2)(0)) + (0 - 4)x + (2 - 4)y\right]$$

$$\Rightarrow N_i^e(3,2) = 0$$

$$N_j^e(x,y) = \frac{1}{16}\left[((2)(0) - (0)(4)) + (4 - 0)x + (0 - 2)y\right]$$

$$\Rightarrow N_j^e(3,2) = \frac{8}{16} = \frac{1}{2}$$

2.3.1. Discharge or recharge point in triangular mesh

Fig. (6-a) shows a triangular element with three nodes at its corners. The coordinates of nodes i, j, and m are (0,0), (4,0), and (2,4), respectively. The area of the triangle is equal to 8 according to equation (1). The shape function for triangular element as given in the equation (2).

$$N_m^e(x,y) = \frac{1}{16}\left[((0)(0) - (4)(0)) + (0 - 0)x + (4 - 0)y\right]$$

$$\Rightarrow N_m^e(3,2) = \frac{8}{16} = \frac{1}{2}$$

So, the pumping rate for three nodes will be equal to:

$$Q = 12\begin{Bmatrix} 0 \\ \dfrac{1}{2} \\ \dfrac{1}{2} \end{Bmatrix} = \begin{Bmatrix} 0 \\ 6 \\ 6 \end{Bmatrix} \begin{matrix} i \\ j \\ m \end{matrix}$$

In the third case, the well is assumed to be located inside the element, with coordinates (2, 2). In this case, according to equation (2), for each of the shape functions, we will have:

$$N_i^e(x,y) = \frac{1}{16}\left[((4)(4) - (2)(0)) + (0 - 4)x + (2 - 4)y\right]$$

$$\Rightarrow N_i^e(2,2) = \frac{4}{16} = \frac{1}{4}$$

$$N_j^e(x,y) = \frac{1}{16}\left[((2)(0) - (0)(4)) + (4 - 0)x + (0 - 2)y\right]$$

$$\Rightarrow N_j^e(2,2) = \frac{4}{16} = \frac{1}{4}$$

$$N_m^e(x,y) = \frac{1}{16}\left[((0)(0) - (4)(0)) + (0 - 0)x + (4 - 0)y\right]$$

$$\Rightarrow N_m^e(2,2) = \frac{8}{16} = \frac{2}{4}$$

So, the pumping rate for three nodes will be equal to:

$$Q = 12\begin{Bmatrix} \dfrac{1}{4} \\ \dfrac{1}{4} \\ \dfrac{2}{4} \end{Bmatrix} = \begin{Bmatrix} 3 \\ 3 \\ 6 \end{Bmatrix} \begin{matrix} i \\ j \\ m \end{matrix}$$

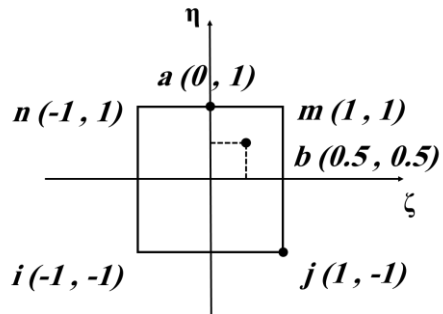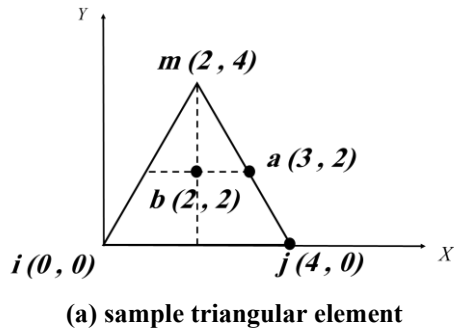So, the pumping rate of each well should be divided between the nodes of that element, depending on its location.

(a) sample triangular element

(b) sample rectangular (squar) element
Fig. 6. A sample triangular element with specified coordinates

It is important to note that if a well is placed on a node of an element, or on an edge of that element, or inside it, the pumping rate is considered only for that element, and in other elements its value is zero. To clarify the issue, consider Fig. 7, where four triangular elements are placed side by side and joining at node 4.
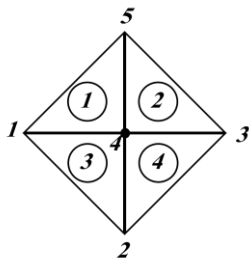

Fig. 7. Patch of four elements joining at node 4

In this case, the rate of pumping well, which was 12 m³/day, is considered only in element number 2 and is considered equal to zero in the other elements, so we have:

$$Q^{e=1} = \begin{Bmatrix} 0 \\ 0 \\ 0 \end{Bmatrix} \begin{matrix} i=1 \\ j=4 \\ m=5 \end{matrix} \quad Q^{e=2} = \begin{Bmatrix} 0 \\ 0 \\ 12 \end{Bmatrix} \begin{matrix} i=3 \\ j=5 \\ m=4 \end{matrix}$$

$$Q^{e=3} = \begin{Bmatrix} 0 \\ 0 \\ 0 \end{Bmatrix} \begin{matrix} i=2 \\ j=4 \\ m=1 \end{matrix} \quad Q^{e=4} = \begin{Bmatrix} 0 \\ 0 \\ 0 \end{Bmatrix} \begin{matrix} i=4 \\ j=2 \\ m=3 \end{matrix}$$

Furthermore, the pumping rate can be distributed among the four elements connected to the node. Thus, it can be expressed as:

$$Q^{e=1} = \begin{Bmatrix} 0 \\ 12/4 \\ 0 \end{Bmatrix} \begin{matrix} i=1 \\ j=4 \\ m=5 \end{matrix} \quad Q^{e=2} = \begin{Bmatrix} 0 \\ 0 \\ 12/4 \end{Bmatrix} \begin{matrix} i=3 \\ j=5 \\ m=4 \end{matrix}$$

$$Q^{e=3} = \begin{Bmatrix} 0 \\ 12/4 \\ 0 \end{Bmatrix} \begin{matrix} i=2 \\ j=4 \\ m=1 \end{matrix} \quad Q^{e=4} = \begin{Bmatrix} 12/4 \\ 0 \\ 0 \end{Bmatrix} \begin{matrix} i=4 \\ j=2 \\ m=3 \end{matrix}$$

2.3.2. Discharge or recharge point in triangular mesh

Three cases are examined for the rectangular (square) element. In the first case, the well is placed at node *j*. In the second case, it is positioned on the upper side of the element, between nodes m and n, at coordinates (0,1). In the third case, it is positioned within the element at coordinates (0.5,0.5) (Fig. 6b). The shape function for the rectangular element is provided in Eq. (3).

$$\tilde{N}_i^e(\xi,\eta) = \frac{1}{4}(1-\xi)(1-\eta)$$

$$\tilde{N}_j^e(\xi,\eta) = \frac{1}{4}(1+\xi)(1-\eta)$$

$$\tilde{N}_m^e(\xi,\eta) = \frac{1}{4}(1+\xi)(1+\eta) \qquad (3)$$

$$\tilde{N}_n^e(\xi,\eta) = \frac{1}{4}(1-\xi)(1+\eta)$$

In the first case, by considering equation (3) for each of the shape functions we have:

$$\tilde{N}_i^e(1,-1) = \frac{1}{4}(1-(1))(1-(-1)) = \frac{1}{4}(0)(2) = 0$$

$$\tilde{N}_j^e(1,-1) = \frac{1}{4}(1+(1))(1-(-1)) = \frac{1}{4}(2)(2) = 1$$

$$\tilde{N}_m^e(1,-1) = \frac{1}{4}(1+(1))(1+(-1)) = \frac{1}{4}(2)(0) = 0$$

$$\tilde{N}_n^e(1,-1) = \frac{1}{4}(1-(1))(1+(-1)) = \frac{1}{4}(0)(0) = 0$$

So, the pumping rate for four nodes will be equal to:

$$Q = 12 \begin{Bmatrix} 0 \\ 1 \\ 0 \\ 0 \end{Bmatrix} = \begin{Bmatrix} 0 \\ 12 \\ 0 \\ 0 \end{Bmatrix} \begin{matrix} i \\ j \\ m \\ n \end{matrix}$$

In the second case, that the location of the well is on the upper edge of the element by considering equation (3) for each of the shape functions we will have:

$$\tilde{N}_i^e(0,1) = \frac{1}{4}(1-(0))(1-(1)) = \frac{1}{4}(1)(0) = 0$$

$$\tilde{N}_j^e(0,1) = \frac{1}{4}(1+(0))(1-(1)) = \frac{1}{4}(1)(0) = 0$$

$$\tilde{N}_m^e(0,1) = \frac{1}{4}(1+(0))(1+(1)) = \frac{1}{4}(1)(2) = \frac{2}{4}$$

$$\tilde{N}_n^e(0,1) = \frac{1}{4}(1-(0))(1+(1)) = \frac{1}{4}(1)(2) = \frac{2}{4}$$

So, the pumping rate for four nodes will be equal to:

$$Q = 12 \begin{Bmatrix} 0 \\ 0 \\ 0.5 \\ 0.5 \end{Bmatrix} = \begin{Bmatrix} 0 \\ 0 \\ 6 \\ 6 \end{Bmatrix} \begin{matrix} i \\ j \\ m \\ n \end{matrix}$$

In the third case, the following is obtained:

$$\tilde{N}_i^e(0.5, 0.5) = \frac{1}{4}(1-(0.5))(1-(0.5))$$

$$= \frac{1}{4}(0.5)(0.5) = \frac{1}{16}$$

$$\tilde{N}_j^e(0.5, 0.5) = \frac{1}{4}(1+(0.5))(1-(0.5))$$

$$= \frac{1}{4}(1.5)(0.5) = \frac{3}{16}$$

$$\tilde{N}_m^e(0.5, 0.5) = \frac{1}{4}(1+(0.5))(1+(0.5))$$

$$= \frac{1}{4}(1.5)(1.5) = \frac{9}{16}$$

$$\tilde{N}_n^e(0.5, 0.5) = \frac{1}{4}(1-(0.5))(1+(0.5))$$

$$= \frac{1}{4}(0.5)(1.5) = \frac{3}{16}$$

So, the pumping rate for four nodes will be equal to:

$$Q = 12 \begin{Bmatrix} \frac{1}{16} \\ \frac{3}{16} \\ \frac{9}{16} \\ \frac{3}{16} \end{Bmatrix} = \begin{Bmatrix} \frac{12}{16} \\ \frac{36}{16} \\ \frac{108}{16} \\ \frac{36}{16} \end{Bmatrix}$$

Here, like the triangular element, in a patch of elements with a common node, if the well coincide with a node, the pumping rate value is considered only for one element, and in other elements its value is zero.

3. Results and Discussion
### 3.1. The results of approach 1
The hypothetical aquifer has been investigated using finite element. The results of groundwater flow modeling in unconfident aquifer and confident aquifer for 5 years are presented in Fig. (8) and Fig. (9). The head distribution in the rectangular and triangular meshes can be observed in Figs. 8(a) and 9(a), and Figs. 8(b) and 9(b), respectively.

Comparison of results obtained with triangular and square meshes. The head contours indicate the spatial distribution of hydraulic heads, showing higher values near recharge wells and lower values near pumping wells, which demonstrates the influence of well locations on flow patterns.

3.2. The results of approach 2
The hypothetical aquifer has been investigated using finite element. The results of groundwater flow modeling in unconfident aquifer and confident aquifer for 5 years are presented in Fig. (10) and Fig. (11). The head distribution in the rectangular and triangular meshes is illustrated in Figs. 10(a) and 11(a), and Figs. 10(b) and 11(b), respectively.

Comparison of results obtained with triangular and square meshes. The contour lines around pumping wells are smoother in Approach 2, indicating a more accurate representation of hydraulic heads and demonstrating the improved performance of this approach. Also, Head value in the nearest neighboring node of wells for unconfident aquifer and confident aquifer presented in Table (2) and Table (3), repectively.
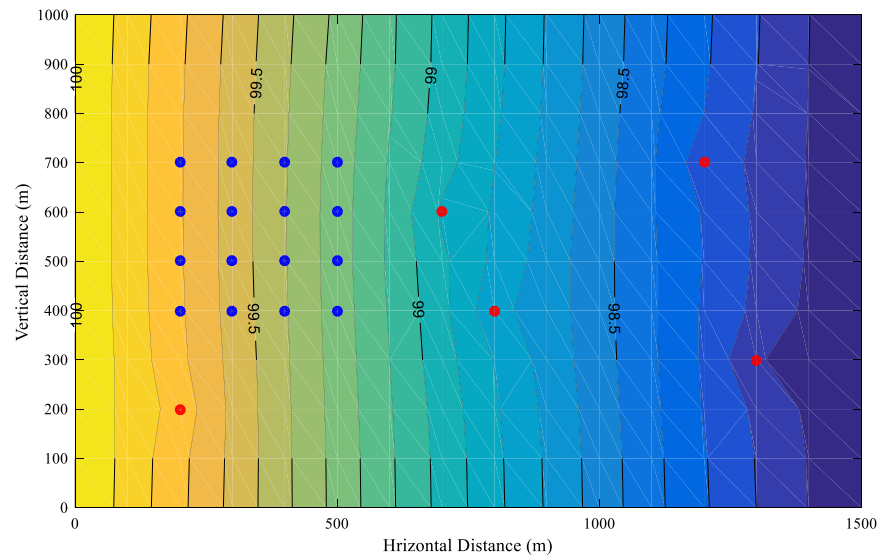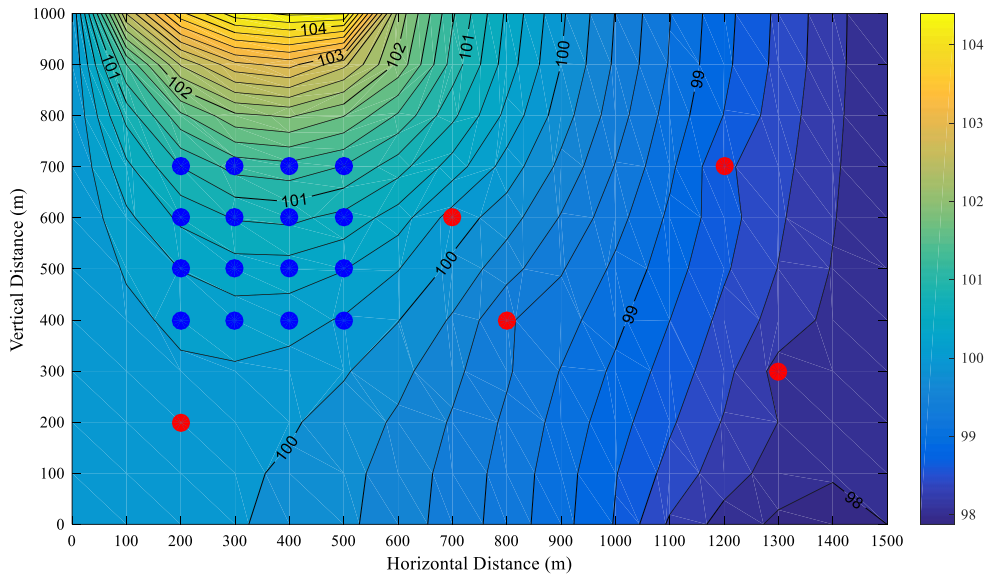
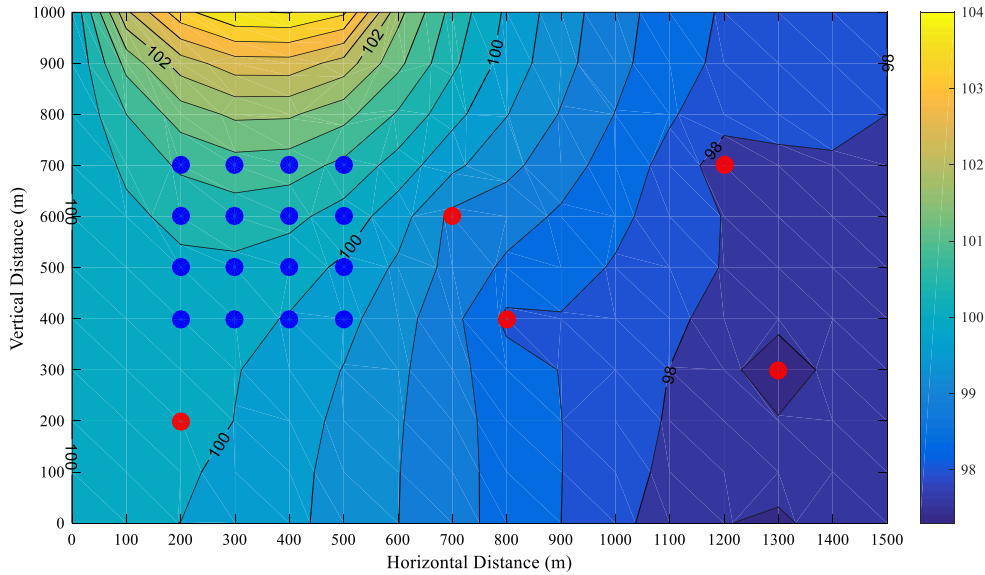**(a) Rectangular (squar) Mesh**
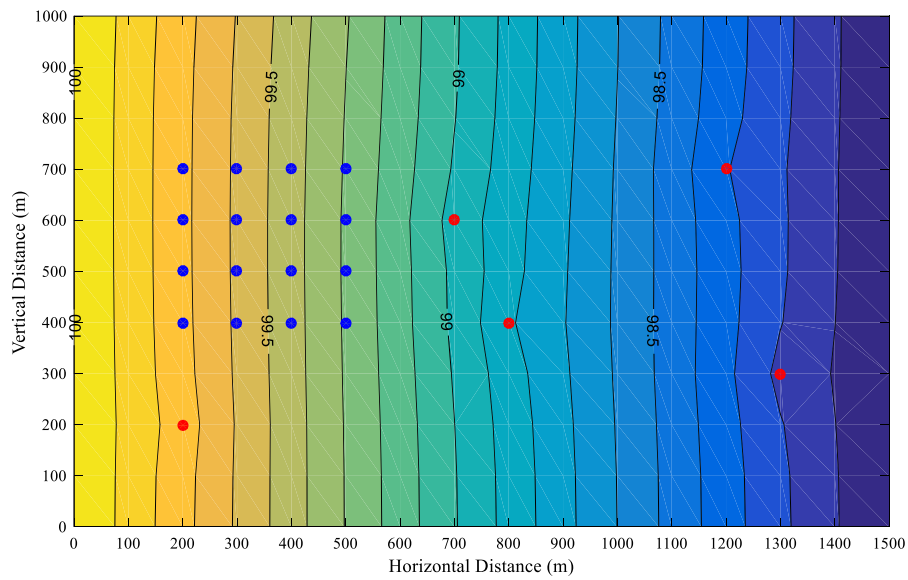
(b) Triangular Mesh
Fig. 8. Groundwater head in unconfident aquifer in approach 1
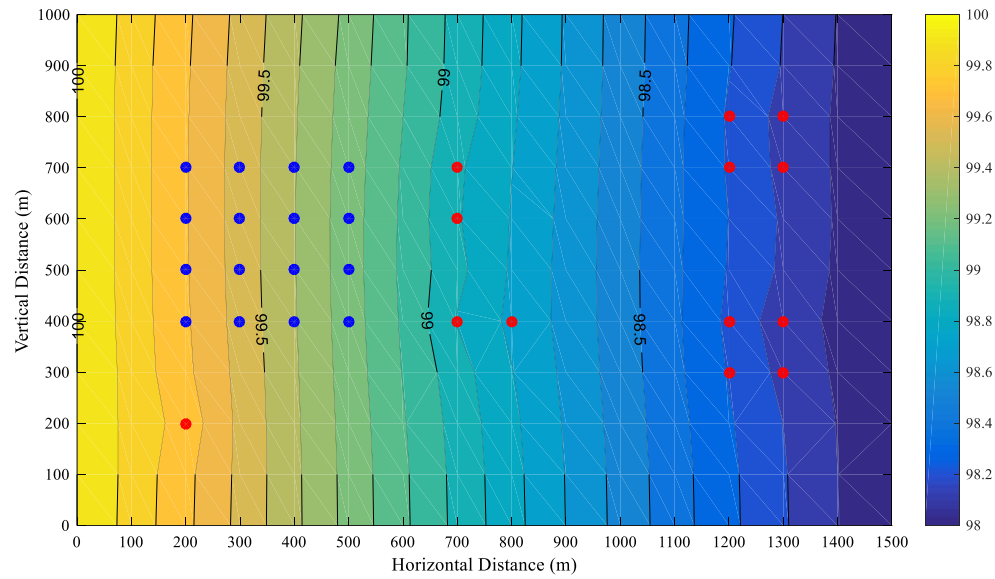
(a) Rectangular (squar) Mesh

(b) Triangular Mesh
Fig. 9. Groundwater head in confident aquifer in approach 1

(a) Rectangular (squar) Mesh

(b) Triangular Mesh
Fig. 10. Groundwater head in unconfident aquifer in approach 2
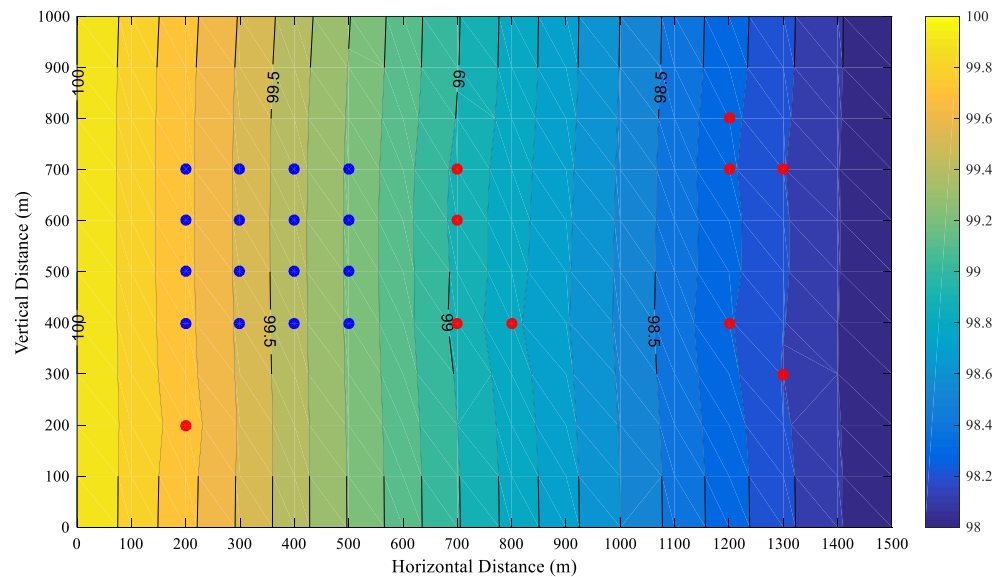
(a) Rectangular (squar) Mesh

(b) Triangular Mesh
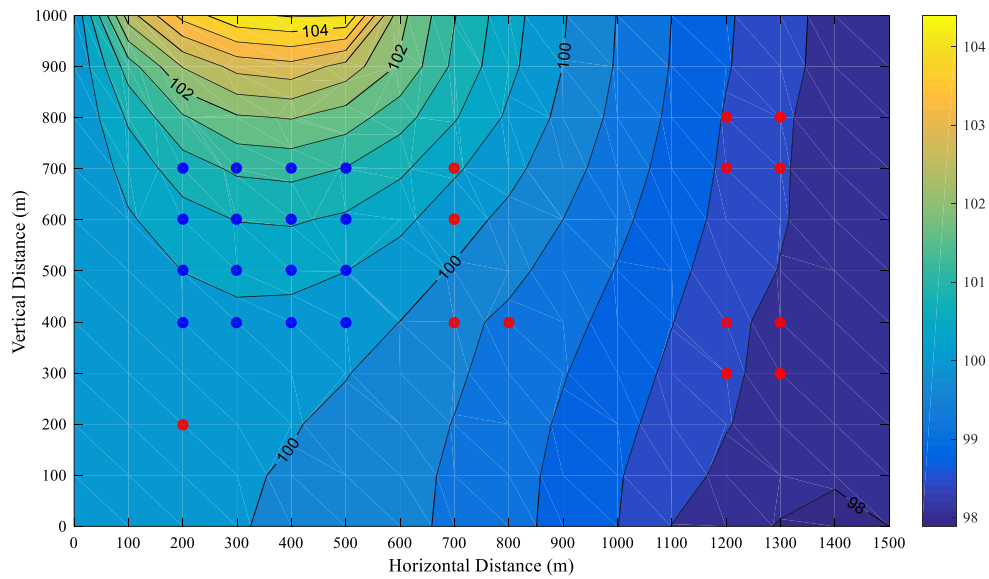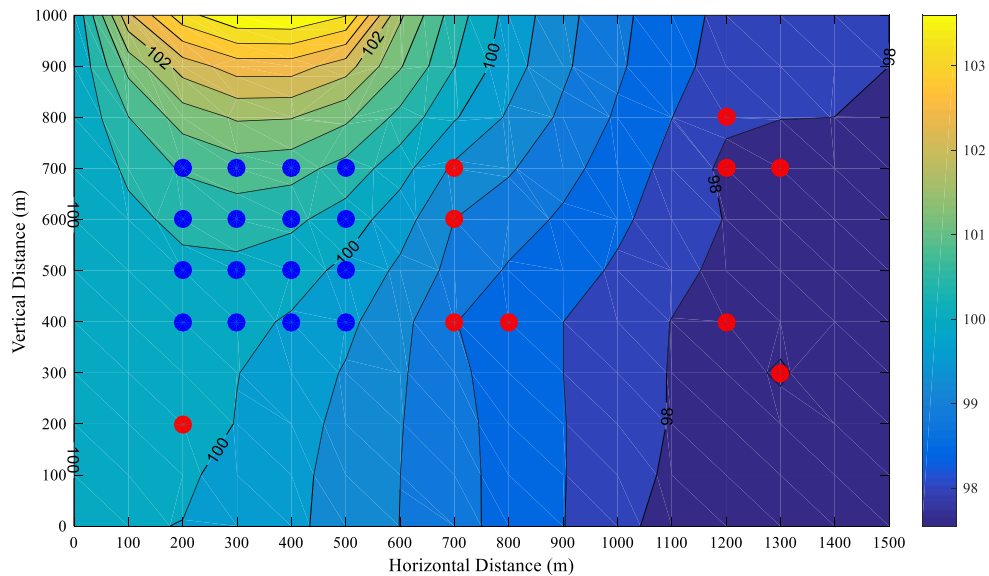**Fig. 11.** Groundwater head in confident aquifer in approach 2

Table 2. Head value in the nearest neighboring node for unconfident aquifer

Well	Node Number	Approach 1		Approach 2			
		Triangular Mesh	Rectangular Mesh	Triangular Mesh	Rectangular Mesh		
		Col (1)	Col (2)	Col (3)	Col (4)	Col (5)= abs(Col (1)- Col (3))	Col (6)= abs(Col (2)- Col (4))
W0	25	99.7489	99.7592	99.7483	99.7587	0.0006	0.0005
W1	82	98.9796	98.9299	98.9721	98.8934	0.0075	0.0365
	93	98.8135	98.7283	98.8218	98.7776	0.0083	0.0493
W2	84	98.9614	98.8835	98.9701	98.9087	0.0086	0.0253
	85	98.9900	98.9420	98.9754	98.9166	0.0145	0.0254
W3	136	98.3237	98.2867	98.3243	98.2922	0.0006	0.0055
	137	98.3297	98.2868	98.3090	98.2779	0.0207	0.0089
	147	98.1728	98.1047	98.1940	98.1710	0.0212	0.0663
	148	98.2046	98.1761	98.2044	98.1399	0.0002	0.0361
W4	140	98.3064	98.2410	98.3171	98.2896	0.0106	0.0485
	141	98.3342	98.3002	98.3268	98.2874	0.0074	0.0127
	151	98.2128	98.1868	98.2046	98.1727	0.0081	0.0141
	152	98.2212	98.1922	98.2156	98.1661	0.0056	0.0261

In the case of the rechage well located at node number 25, the first and second approaches have the same definition, and as can be seen in the Table (2), the difference between the two approaches is very small. However, when a square mesh is used, the first and second approaches have a large difference. This contrasts with the triangular mesh, where the difference between the two approaches is small and either approach is acceptable. Therefore, if the study area model is to be simplified and the pumping well is transferred to the nearest node, this action is justified only when triangular gridding is used. Also, when square elements are used to grid the model area, the second approach should be employed. Otherwise, the modeling error rate increases. Although it is generally recommended that the second approach is always used to reduce the error rate of groundwater flow modeling.

As can be seen in the Table (3), when triangular gridding is used, the first and second approaches have a significant difference. However, when square mesh is used, the difference between the two approaches is negligible and the use of either approach is acceptable. Beside, in the triangular element, the first approach calculates more head values

in all nodes than the second approach, except for the head in the node where the well is located, and this causes the head value in the surrounding nodes to be estimated more than the actual value. On this basis, in a confined aquifer when using a triangular element, it is still recommended to use the second approach. In MODFLOW, wells are represented as specified fluxes applied to model cells. Thus, pumping is distributed over the cell volume, and the computed head reflects the average cell head rather than the actual wellbore head. This approach is essentially the one examined in the present article and is therefore considered more accurate and appropriate than simply relocating wells to the nearest grid cell. Table 4 summarizes the quantitative error metrics between Approach 1 and Approach 2 for both unconfined and confined aquifers and for triangular and rectangular meshes. MAE, RMSE, and maximum absolute error are provided to give a clear numerical assessment of model performance.

The results indicate that Approach 2 significantly improves accuracy, particularly in the confined aquifer with triangular mesh, where the differences are largest using the nearest node approach.

Table 3. Head in the nearest neighboring node for confident aquifer

Well	Node Number	Approach 1		Approach 2			
		Triangular Mesh	Rectangular Mesh	Triangular Mesh	Rectangular Mesh		
		Col (1)	Col (2)	Col (3)	Col (4)	Col (5)= abs(Col (1)- Col (3))	Col (6)= abs(Col (2)- Col (4))
W0	25	100.2672	100.1675	100.2603	100.1666	0.0069	0.0009
W1	82	99.9144	99.7754	98.8251	99.7032	1.0893	0.0722
	93	99.3096	99.4215	98.4081	99.5189	0.9015	0.0974
W2	84	100.0955	100.1117	99.1979	100.1617	0.8976	0.0500
	85	100.6924	100.5073	99.5196	100.4570	1.1728	0.0503
W3	136	97.7375	98.4654	97.7444	98.4761	0.0069	0.0107
	137	97.8814	98.5429	97.6371	98.5255	0.2443	0.0174
	147	97.3023	98.1267	97.5521	98.2568	0.2498	0.1301
	148	97.7327	98.3246	97.7301	98.2536	0.0026	0.0710
W4	140	97.7833	98.6360	97.9085	98.7313	0.1252	0.0953
	141	98.1528	98.7940	98.0654	98.7689	0.0874	0.0251
	151	97.9481	98.4685	97.8521	98.4409	0.0960	0.0276
	152	98.0732	98.5055	98.0068	98.4543	0.0664	0.0512

Table 4. Quantitative Statistical Measures for Triangular and Rectangular Meshes in Unconfined and Confined Aquifers

Aquifer Type	Mesh Type	MAE	RMSE	Max Absolute Error
Unconfined	Triangular	0.0087	0.0109	0.0212
Unconfined	Rectangular	0.0273	0.0331	0.0663
Confined	Triangular	0.3805	0.5777	1.1728
Confined	Rectangular	0.0537	0.0652	0.1301

4. Conclusion

In the modeling of groundwater flow and contaminant transport, numerical methods such as finite difference and finite elements (triangular and rectangular elements) are used. In these modeling, whether the aquifer is hypothetical or real, there are always recharge or discharge wells as point source or a sink. In dealing with this point source, a simple approach is to transfer the recharge or discharge well to the nearest node after discretizing the model domain. In this case, if several wells are close to a node, they are all assigned to that node, and their pumping rates are subsequently summed. Besides, to avoid such a discrepancy, irregular mesh or smaller regular mesh can be used to ensure that all wells coincide on the nodes. However, it should be noted that using a finer mesh increases the computational cost.

Therefore, in this study, a different approach was used in dealing with pumping wells. In this approach, regardless of the type of element (triangular or rectangular (square)), there are three cases. In the first case, the well is exactly coincide on the node. In the second case, the well is exactly on the edge of an element, and in the third case, the well is inside the element. In the first case, the well coincides exactly with a node, which is identical to the first approach. However, in the second and third cases, the value of the interpolating function is calculated according to the coordinates of the well and the coordinates of the nearest neighboring nodes, and the pumping rate value is divided among those nodes.

In this study, a hypothetical aquifer was investigated and an attempt was made to include all the characteristics of an aquifer, such as different hydraulic conductivity in different parts of the aquifer, application of distributed source and point source and sink, boundary conditions of a specific head (Dirichlet condition), a specific and no-flow boundary (Neuman condition). This aquifer was also investigated under two conditions: unconfined and confined aquifers.

The study demonstrated that Approach 2 provides a more accurate representation of hydraulic heads compared to the nearest node method. Quantitative error metrics indicate that for unconfined aquifers, the mean absolute error (MAE) is as low as 0.0088 for triangular meshes and 0.0273 for rectangular meshes, with maximum errors of 0.0212 and 0.0663, respectively. In confined aquifers, the improvements are more pronounced, particularly for triangular meshes, where MAE reaches 0.3805 and maximum error 1.1728, whereas rectangular meshes exhibit MAE of 0.0538 and maximum error of 0.1301.

Based on these results, for unconfined aquifers, the difference between the two approaches is negligible when triangular meshes are used, allowing wells to be transferred to the nearest node without significant error. However, for unconfined aquifers with square meshes, as well as for confined aquifers with either triangular or square meshes, distributing the pumping rate among neighboring nodes (Approach 2) is recommended to reduce modeling errors.

In confined aquifers with triangular meshes, transferring wells to the nearest node tends to overestimate hydraulic heads in surrounding nodes, whereas Approach 2 provides a more accurate representation. Finally, if the study area model is to be simplified by transferring pumping wells to the nearest node, this is justified only for unconfined aquifers with triangular grids. For all other cases, Approach 2 is recommended. For future work, applying this methodology to real-world aquifers, including transient conditions and multi-layered systems, could further enhance its applicability and robustness.

5. Acknowledgment

6. Conflict of Interest

The authors declare that there is no conflict of interest.

7- References

Akbarpour, A., Zeynali, M. J., & Tahroudi, M. N. (2020). Locating optimal position of pumping Wells in aquifer using meta-heuristic algorithms and finite element method. *Water Resources Management*, *34*(1), 21-34.

Eldho, T. I., & Swathi, B. (2018). Groundwater contamination problems and numerical simulation. Environmental Contaminants: Measurement, Modelling and Control, 167-194.

Ghafouri, H. R., & Darabi, B. S. (2007). Optimal identification of ground-water pollution sources. *International Journal of Civil Engineering*, *5*(2), 144-156.

Guneshwor L, Eldho TI, Kumar AV (2018). Identification of Groundwater Contamination Sources Using Meshfree RPCM Simulation and Particle Swarm Optimization. Water Resources Management, 32(4): 1517-1538.

Istok, J. D. (1989). Groundwater modeling by the finite element method (Vol. 13, p. 132). Washington, DC: American Geophysical Union.

Jafarzadeh, A., Pourreza-Bilondi, M., Akbarpour, A., Khashei-Siuki, A., & Azizi, M. (2023). Sensitivity and stability analysis for groundwater numerical modeling: a field study of finite element application in the arid region. *Acta Geophysica*, *71*(2), 1045-1062.

Koch, T., Helmig, R., & Schneider, M. (2020). A new and consistent well model for one-phase flow in anisotropic porous media using a distributed source model. *Journal of Computational Physics*, *410*, 109369.

Kumar D, Ch S, Mathur S, Adamowski J (2015). Multi-objective optimization of in-situ bioremediation of groundwater using a hybrid metaheuristic technique based on differential evolution, genetic algorithms and simulated annealing. Journal of Water and Land Development, 27(1), 29-40.

Lozano Hernández, B. L., Marín Celestino, A. E., Martínez Cruz, D. A., Ramos Leal, J. A., Hernández Pérez, E., García Pazos, J., & Almanza Tovar, O. G. (2024). A systematic review of the current state of numerical groundwater modeling in American Countries: Challenges and future research. *Hydrology*, *11*(11), 179.

Mategaonkar, M., Eldho, T. I., & Kamat, S. (2018). In-situ bioremediation of groundwater using a meshfree model and particle swarm optimization. Journal of Hydroinformatics, 20(4), 886-897.

Mohtashami A, Akbarpour A, Mollazadeh M (2017). Development of two-dimensional groundwater flow simulation model using meshless method based on MLS approximation function in unconfined aquifer in transient state. Journal of Hydroinformatics, 19(5), 640-652.

Reilly, T. E., & Harbaugh, A. W. (2004). *Guidelines for evaluating ground-water flow models*. DIANE Publishing.

Sharief, S. M. V., Eldho, T. I., Rastogi, A. K., & Gurunadha Rao, V. V. S. (2012). Optimal groundwater remediation by pump and treat using FEM-and EGA-based simulation-optimization model. Journal of Hazardous, Toxic, and Radioactive Waste, 16(2), 106-117.

Singh, K. G., & Pathania, T. (2025). Development and real field application of meshless generalized finite difference method for unconfined groundwater flow modelling. *Mathematics and Computers in Simulation*.

Vellando, P., Juncosa, R., Padilla, F., & García-Rábade, H. (2020). Numerical evaluation of groundwater flows: MODFLOW vs. FE models. *Journal of Porous Media*, *23*(6).

Zeynali, M. J. , Nazeri Tahroudi, M. and Mohammadrezapour, O. (2024). Investigating the Optimization-Simulation Problem of Groundwater Remediation Under Various Scenarios. *Water Harvesting Research*, *7*(1), 125-139.

Zeynali, M. J. , Nazeri Tahroudi, M. and Mohammadrezapour, O. (2024). Optimizing Pump-and-Treat Method by Using Optimization-Simulation Models. *Sustainable Earth Trends*, *4*(3), 19-30. doi: 10.48308/set.2024.236332.1060

Zeynali, M. J., Pourreza-Bilondi, M., Akbarpour, A., Yazdi, J., & Zekri, S. (2022). Optimizing pump-and-treat method by considering important remediation objectives. *Applied Water Science*, *12*(12), 268.

Zeynali, M. J., Pourreza-Bilondi, M., Akbarpour, A., Yazdi, J., & Zekri, S. (2022). Development of a contaminant concentration transport model for sulfate-contaminated areas. *Applied Water Science*, *12*(7), 169.